Vol. 25, No. 1(2026) Poly26662

Revista Mexicana de Ingeniería Química

A model for describing experimental data from polymerization reactions of binary mixtures of monomers

Un modelo para describir datos experimentales de reacciones de polimerización de mezclas binarias de monómeros

E.Y. Calvillo-Muñoz[1], N. V. Likhanova[1], I. V. Lijanova[2], F. de J. Guevara-Rodríguez[1*]

[1] Instituto Mexicano del Petróleo, Eje Central Lázaro Cárdenas 152, San Bartolo Atepehuacan, Ciudad de México, 07730, México.

[2] Instituto Politécnico Nacional, CIITEC, Cerrada Cecati S/N, Colonia Santa Catarina de Azcapotzalco, Ciudad de México, 02250, México.

Received: September 5, 2025; Accepted: December 5, 2025

Abstract

In the present work, three binary mixtures, derived from acrylamide (*AM*), vinylpyrrolidone (*VP*), and vinylbenzyl trimethylammonium chloride (*VBTA*), were synthesized to form ionic copolymers through the inverse microemulsion method. A mathematical model is proposed to describe the heat flow derived from thermoanalytical data of a binary polymerization reaction, utilizing the Differential Scanning Calorimetry (DSC) technique. In the initial stage, the monomer conversion function model is proposed to describe the experimental data derived from Nuclear Magnetic Resonance (NMR). Subsequently, in the second and final stage, a calorimetric model (based on the previously derived conversion function and the molar fraction of each component) is proposed to describe the heat flow data from polymerization reactions of binary mixtures of monomers.

Keywords: Calorimetry data, polymerization reaction, monomer conversion, heat flow.

Resumen

En el presente trabajo, se sintetizaron tres mezclas binarias, derivadas de acrilamida (*AM*), vinilpirrolidona (*VP*) y cloruro de vinilbenciltrimetilamonio (*VBTA*), para formar copolímeros iónicos mediante el método de microemulsión inversa. Se propone un modelo matemático para describir el flujo de calor derivado de los datos termoanalíticos de una reacción de polimerización binaria, utilizando la técnica de Calorimetría Diferencial de Barrido (DSC). En la etapa inicial, se propone el modelo de la función de conversión de monómeros para describir los datos experimentales derivados de Resonancia Magnética Nuclear (RMN). Posteriormente, en la segunda y última etapa, se propone un modelo calorimétrico (basado en la función de conversión derivada previamente y la fracción molar de cada componente) para describir los datos de flujo de calor de las reacciones de polimerización de mezclas binarias de monómeros.

Palabras clave: Datos de calorimetría, reacción de polimerización, conversión de monómeros, flujo de calor.

*Corresponding author. *E-mail*: fguevara@imp.mx ;

https://doi.org/10.24275/rmiq/Poly26662

ISSN:1665-2738, *issn-e*: 2395-8472

1 Introduction

Over the past two decades, scientific interest in obtaining ionic macromolecules with positive, negative, or zwitterionic properties has surged due to their unique characteristics, including high ionic conductivity, high viscosity in saline media, and temperature resistance (Wang, 2012), (Sadeghalvaad, 2015). These macromolecules possess the ability to incorporate water-soluble ionic compounds, such as vinylbenzyl trimethylammonium chloride, which enhance their polymeric chain properties. Notably, *VBTA* provides tolerance to divalent ions at high temperatures and hydrolysis (Xu, 2014), (Bai, 2015), (Hassan, 2013), enabling the macromolecule to increase its thermal resistance, develop tolerance to saline media, and improve its dissolution capacity in aqueous media (Li, 2017). These advantages make these materials highly sought after and in demand, particularly in the oil industry (Noppakundilograt, 2010).

Synthetic polymers are utilized in diverse technologies due to their exceptional flexibility in the synthesis process and the organization of monomers within the polymeric structure. Furthermore, the escalating complexity of numerous industrial processes and their conditions necessitates the development of novel polymeric substances or materials that can meet contemporary demands (Sheng, 2015), (Jung, 2013), (Wang, 2012). The synthesis and demand for these polymers exert both technological and societal impacts. Consequently, novel approaches have concentrated on enhancing properties to fulfill new requirements (Giles, 2005). Consequently, polymeric structures are modified by incorporating various types of monomers, resulting in the formation of copolymers (Stahl, 2024), (Ferguson, 1979). Copolymers are compounds derived from the incorporation of two distinct types of monomers into the polymeric chain. They are typically designed when the homopolymer fails to meet the requirements or properties of a specific application (Shrivastava, 2018), (Mazrouaa, 2013), (Gaillard, 2010). Like homopolymers, copolymers can be synthesized employing diverse synthesis methods, each with distinct advantages and tailored to the characteristics of the final material (Choonara, 2011), (Lu, 2009).

Water-soluble synthetic polymers stable under high salinity conditions (greater than 250,000 ppm of total dissolved solids) and temperatures greater than 130°C are of high interest to the Mexican oil industry for their possible application in the processes of additional oil recovery and the preparation of chemical compositions for water control in oil-producing wells. The synthesis procedure of copolymers involves the polymerization reaction that generates a macromolecule. However, the primary challenge in polymer synthesis lies in the selection of appropriate methods and techniques. These methodologies and techniques encounter significant limitations, including the concentration and incorporation of monomers, heat dissipation within the reaction matrix, and solution viscosity (Adumitrchioaie, 2018), (Hamzehlou, 2020), (Gu, 2005). These factors directly impact the desired properties of the macromolecules, which, in turn, influence the final application (Namazi, 2017), (Hao, 2005).

In this context, emulsion copolymerization and even liquid crystalline phase copolymerization are effective methods for incorporating ionic monomers into the main polymer chain, resulting in the formation of ionic polymers with a reduced polydispersity degree and enhanced molecular weight (Qiu, 2008). Notably, the inverse microemulsion method facilitates the integration of water-soluble monomers, such as acrylamide, vinylpyrrolidone, and Ionic Liquids (ILs), including *VBTA*, which contribute to system stability. However, it is important to note that this method entails an increase in the anisotropy degree of the polymer formation, as each monomer exhibits distinct reactivity (Singh, 1994), (Ianchis, 2014). The complexity of the system necessitates meticulous analysis, where challenges, such as data processing, must be overcome through the utilization of mathematical models, normalizations, statistical treatment of deconvolutions, and even fitting techniques, including square methods. These approaches enable the appropriate projection of the reaction progress (Colmán, 2016), (Colmán, 2014), (Silva, 2011).

Since 1994, the method developed by Fineman and Ross was utilized to determine the reactivity of *AM* and *VP* in inverse microemulsions (Singh, 1994). In another approach, the conversion of monomers into polymerization reactions with inverse emulsion is considered a first-order process. The primary challenges in this type of reaction include the kinetic polymerization, the evolution of polymer weight, and the simultaneous action of an “intrinsic” initiator (Alb, 2006). Subsequently, models developed by Ugelstad/O’Toole, Nomura, and Gilbert were employed to determine the velocity constants for copolymerization of *AM* and butyl-acrylate under inverse microemulsions (Yildiz, 2007). Moreover, the monomer conversion of *AM* and the number of particles were described with a model developed for a polymeric reaction in an inverse microemulsion with controlled propagation at high conversion (Torraga, 2021). Recently, mechanistic models were developed to describe the global and individual monomer conversion, the final molecular weight of the polymeric product, the polymerization rate, the size distribution, the conversion velocity, and

other properties of inverse emulsions containing *AM*, styrene, and anhydric maleic acid (Moghaddam, 2025). Despite these significant contributions, our proposed model is based on the empirical monomer conversion formula and the concept of distribution of monomers with a free radical, the latter being the basis for the calorimetry model. The model represents a mesoscopic view rather than a microscopic view, a focus that has not been previously explored.

The goal of the work is to find an efficient way to obtain polymer using a calorimetric mathematical model for monitoring and quantifying the monomer conversion in polymerization reactions. In this work, the progress of the polymerization reaction by the inverse emulsion method for three binary systems, namely *AM-VBTA*, *VBTA-VP*, and *VP-AM*, was monitored by NMR and DSC techniques. The data from this monitoring were fed into a calorimetric mathematical model, which was developed to describe the heat flow of the polymerization reactions.

2 Monomer conversion

2.1 Laboratory details

2.1.1 Materials

Analytical grade reagents were acquired from Sigma-Aldrich. The employed monomers were acrylamide (*AM*, 98%), N-vinylpyrrolidone (*VP*, 99%) and vinylbenzyl trimethylammonium chloride (*VBTA*, 99%); azobisisobutyronitrile (*AIBN*, 12 *wt.%* in acetone) was used as initiator; cyclohexane (99%) was the continuous phase of the inverse emulsion, and polyoxyethylene isooctylphenyl ether (Igepal® ca 720) and sorbitan monooleate (Span® 80) were the emulsifiers.

2.1.2 Inverse microemulsion preparation

The synthesis of three distinct copolymers *AM-VBTA*, *VBTA-VP*, *VP-AM* was accomplished employing the inverse emulsion method, as outlined in Table 1. The formulation of microemulsions with an *HLB* of 6.7 and an emulgents concentration of 14.5% comprises two distinct phases: In one phase, the continuous lipophilic phase of the inverse emulsions was meticulously prepared by dissolving 3.3g de Span® 80 in 16mL of cyclohexane. Simultaneously, the second phase, the hydrophilic dispersed phase was meticulously crafted by utilizing 6mL of degassed deuterated water, 1.0g of Igepal® ca 720, and the corresponding monomers, as specified in Table 1. Subsequently, both phases (lipophilic and hydrophilic) were meticulously combined using an Ultra-turrax T25 Basic homogenizer at a rotational speed of 13,000 rpm for 8min. Subsequently, each of the three emulsions, characterized by an average droplet size of 0.1μm, as determined using an AccuSizer 780 AD Autodiluter device, was individually transferred into a three-necked round-bottom flask. Subsequently, the emulsions underwent deaeration through the deliberate introduction of nitrogen gas via bubbling for 30min. Under the continuous presence of nitrogen gas and a constant stirring rate of 350rpm, the initiator *AIBN* (with an initiator mole ratio of 0.007 to the monomers) was meticulously added to each emulsion at a rate of 30mL/h, utilizing a syringe pump. For each emulsion, two distinct samples were collected to monitor the ongoing polymerization reaction.

Table 1. Molar ratio of monomers for each emulsion system.

Synthesized copolymer structures	Monomers	Molar and weight ratios of monomers
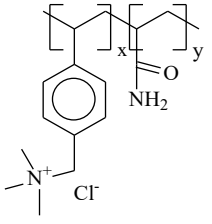	AM-VBTA	AM (0.050 mol (3.575 g)) / VBTA (0.007 mol (1.430 g))
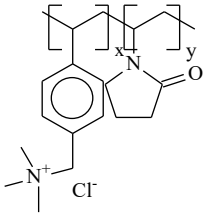	VBTA-VP	VBTA (0.009 mol (2.000 g)) / VP (0.027 mol (3.000 g))

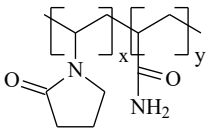

VP-AM VP (0.017 mol (1.878 g)) / AM (0.044 mol (3.130 g))

Table 2. Vinyl groups peaks of monomers taken for monitoring.

Vinyl groups of monomers (quantity of hydrogen atoms)	Structure (the protons of the signals are marked in red)	Peak (region of chemical shift), ppm
AM (2H)	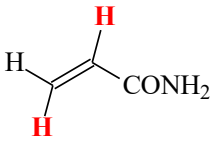	6.13 (5.68-6.53)
VP (1H)	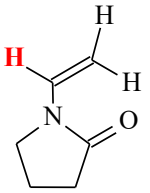	6.88 (6.71-7.25)
VBTA (1H)	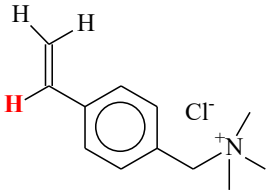	6.60 (6.14-7.02)

2.1.3 *Monitoring of the polymerization reaction by ^1H NMR spectroscopy*

A sample of the formed emulsion was placed (under a nitrogen atmosphere) in a 1.0mL NMR glass tube, which was sealed. The ^{1}H NMR monitoring was performed using a Bruker BioSpin GmbH 600MHz piece of equipment for 4h at a constant temperature of 60°C. The reaction progress spectrum was collected every 15min for each of the three copolymer systems. For each monomer, the peaks for monitoring the monomer conversion in the mixture are represented in Table 2.

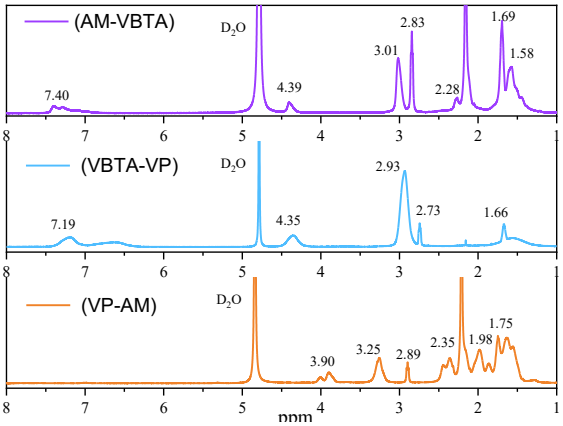

Figure 1. ^{1}H NMR spectra of the obtained copolymers.

2.2 *Mathematical adjustment*

The conversion of monomers into polymers plays a significant role in understanding the evolution of polymeric reactions. The conversion data derived from the polymerization experiment for each monomer in the binary mixture were described through Equation (1), namely,

$$p_\alpha(t) = A_\alpha \; erf\,(a_\alpha t)^{m_\alpha} + (100 - A_\alpha) \; erf\,(b_\alpha t)^{n_\alpha} \quad (1)$$

where α is the monomer label, *i.e.* $\alpha \in \{AM, VP, VBTA\}$, and erf is the error function (Abramowitz, 1972) given by Equation 2:

$$erf(x) = \frac{2}{\sqrt{\pi}} \int_0^x e^{-\tau^2} d\tau \quad (2)$$

The conversion function and its time derivative at $t = 0$ fulfills with $p_\alpha(0) = 0$ and $\dot{p}_\alpha(0) = 0$, and therefore, exponents must be $m_\alpha \geq 2$ and $n_\alpha \geq 2$. Moreover, p_α corresponds to a non-decreasing function; thus, its parameters are $a_\alpha > 0$ and $b_\alpha > 0$. In summary, the monomer-α conversion function p_α has the domain $0 \leq t$, is a continuous function, has no negative values $p_\alpha(t) \geq 0$, is a monotonically non-decreasing

function $\dot{p}_\alpha(t) \geq 0$, and has the limit $p_\alpha(t) \rightarrow 100\%$ at $t \rightarrow \infty$. The adjustment parameters are in the set $S_\alpha = \{A_\alpha, m_\alpha, n_\alpha, a_\alpha, b_\alpha\}$, and are determined by minimizing the mean square deviation between the experimental data and results from the conversion function $p_\alpha(t)$.

2.3 Results

Figure 2 shows experimental data for the conversion of monomers to copolymers, denoted by dot symbols, for the three polymeric reactions: *AM-VBTA*, *VBTA-VP*, and *VP-AM* copolymers. The solid line represents the outcome of Equation 1, applied to each component within the polymeric reaction. The parameter values were determined through the minimization of the mean square deviation between the experimental data and Equation 1; and those values are in Table 3.

In the case of the copolymer *AM-VBTA*, the gradual reaction progress and corresponding conversion of the monomers into polymers were observed. The *VBTA* monomer exhibited a conversion of 24% at the initial reaction stage. However, at 126min, its conversion percentage increased to 94%, indicating the acceleration stage. Finally, 100% conversion was achieved at 160min. Regarding *AM*, the initial percentage was 41%. At the acceleration stage (at 105min), a conversion of 97% was observed, with the maximal conversion occurring at 160min.

In the case of the copolymer *VBTA-VP*, conversions of 57% and 47% were observed for *VP* and *VBTA*, respectively, at 9min and 29min, respectively. The acceleration stage for *VP* occurred at 76min, while for *VBTA*, it happened at 138min, with conversions around 97%. Finally, at 200min, both monomers reached the same speed, achieving 100% conversion.

The copolymer *VP-AM* exhibited an immediate reaction rate, with both monomers reaching conversions of approximately 51% within 2min. While *AM* exhibited a similar onset, it demonstrated increased reactivity after 10min, reaching conversion percentages of 99%. Conversely, the reaction time required by the *VP* monomer was longer than that of *AM* to achieve 100% conversion.

In general, Equation (1) adequately described the monomer conversion observed in the experiment. Notably, the *VP-AM* experiment exhibited a faster monomer conversion rate compared to other cases. Although the experimental data for *VP* monomers appeared scattered, Equation (1) offered useful insights into the conversion behavior. In this case, the deviation indicates that adding more terms to Equation (1) could enhance its multimodal description (Guzmán, 2024). Furthermore, the most rapid monomer chemical reaction was observed in the mixture of *VBTA* (blue dots), *VP* (green dots), and *AM* (red dots). These components exhibited the fastest chemical reactions in the *AM-VBTA*, *VBTA-VP*, and *VP-AM* experiments, respectively.

Table 3. The parameters value of Equation (1), which adequately fits the experimental data of the polymerization reaction.

Copolymer	α	A_α [%]	m_α	n_α	a_α [min^{-1}]	b_α [min^{-1}]
AM-VBTA	*AM*	50.14	2	20.84	0.01282	0.01659
	VBTA	54.88	2	5.742	0.03243	0.01748
VBTA-VP	*VBTA*	53.65	2	2.369	0.04522	0.008702
	VP	53.60	2	2	0.1656	0.02640
VP-AM	*VP*	53.60	2	2	1.0936	0.02176
	AM	53.58	2	2	1.0064	0.2109

3 Calorimetry

3.1 Laboratory details

In the second stage, heat flow data were collected using Differential Scanning Calorimetry (DSC) technology equipped with SETARAM EVO equipment. The equipment calibration was conducted to ensure the precision, comparability, and reproducibility of the temperature and heat flux measurements. The procedure was executed using the standard kit S60/50194. A precise polymer with a concentration of 500mg per standard is utilized, specifically indium, tin, lead, and zinc. For each standard, the temperature of the fusion point is known and is 156.59°C, 231.94°C, 327.47°C, and 419.56°C, respectively. The enthalpy of one of them is calculated from the area under the main peak from the endothermic effect and its base; its value is also known and for each standard corresponds to 28.5 J/g @ In, 60.2 J/g @ Sn, 23.0 J/g @ Pb, and 107.4 J/g @ Zn. The calculated value derived from 5 experiments is compared with those values, and its deviations must be within the range defined by the equipment uncertainty, namely: ± 0.5 J/g.

A sample of the 15μL formed emulsion (as described in 2.1.2 and the *AIBN* initiator) was placed under a nitrogen atmosphere into hermetically sealed aluminum crucibles with a capacity of 30μL. An

isothermal process was conducted at 60°C for a duration of $4h$ to determine the heat released from each of the proposed copolymerization reactions: *AM-VBTA*, *VBTA-VP*, and *VP-AM*. Subsequently, the mathematical fitting was performed, and the correlation between the heat flow data and the conversion data obtained by ^{1}H NMR spectroscopy was observed.

3.2 *Heat flow model*

In Section 2, an empirical formula was introduced to explain monomer conversion during a polymerization reaction. Section 3 builds on this by combining the concept of monomer distribution with a free radical and the earlier empirical formula to develop the heat flow model. The first step is to define $q(t)$ as the heat flow system (in mW unit) at time $t \in [0, t_F]$, where t_F is the final time. For this time interval, the baseline was defined as $q_{base}(t) = (q(t_F) - q(0))\, t/t_F + q(0)$. The baseline gradient and baseline height derived from experimental data are reported in Table 4.

Table 4. Baseline gradient $M = (q(t_F) - q(0))/t_F$, and baseline height $q(0)$ derived from experimental data.

Copolymer	M [mW/min]	q(0) [mW]
AM-VBTA	-1.421	-2.942
VBTA-VP	5.933×10^{-5}	-3.842
VP-AM	9.572×10^{-5}	-3.950

Excess heat flow was defined as $\Delta q(t) = q(t) - q_{base}(t)$ and modeled with Equation 3

$$\Delta q(t) = \int_0^t \rho(\tau)\, Q(t-\tau)\, d\tau \tag{3}$$

Certainly, the model's validity is restricted to the interval $t \in [0, t_F]$. Equation (3) represents the convolution of two functions, namely $\rho(t)$ and $Q(t)$. The former, $\rho(t)$, represents the monomer distribution with a free radical and is modeled using the gamma distribution, as specified in Equation 4, namely,

$$\rho(t) = \frac{\lambda}{\Gamma(z)} (\lambda t)^{z-1} e^{-(\lambda t)} \tag{4}$$

where $\Gamma(z)$ is the gamma function [30]

$$\Gamma(z) = \int_0^\infty t^{z-1} e^{-t}\, dt. \tag{5}$$

Certainly, a monomer with a free radical is generated when its double bond becomes open and is eliminated during the chemical reaction. Consequently, $\rho(t)$ represents the concentration of such monomers with a free radical (in units of $1/min$) within the system.

The gamma distribution is applied here because its valid range aligns with non-negative times, and its shape resembles (though is not identical to) a typical Gaussian distribution. Additionally, the mean value (m) and standard deviation (σ) defining this distribution are provided in the following equations,

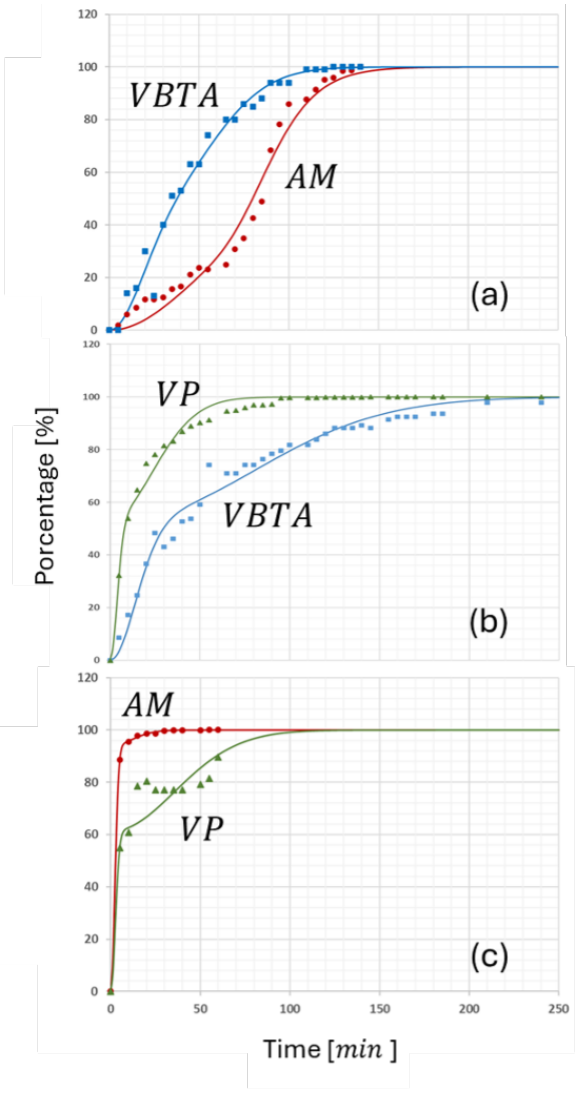

Figure 2. Monomers conversion function in the polymerization reaction: (a) *AM-VBTA*, (b) *VBTA-VP*, and (c) *VP-AM*. Equation (1) is the solid curve, and the dots correspond to experiment data. Red circles, green triangles, and blue squares are associated with *AM*, *VP*, and *VBTA*, respectively.

$$m = \frac{z}{\lambda}; \quad \sigma^2 = \frac{z}{\lambda^2} \tag{6}$$

In Equation (4), z and λ are the parameters. For illustration, Figure 3 depicts the Gamma distribution obtained from the *AM-VBTA* polymerization reaction. This function reached its peak number of active sites at approximately 36min. Subsequently, the number of free monomers declined over time, consequently leading to a reduction in the density of monomers with a free radical.

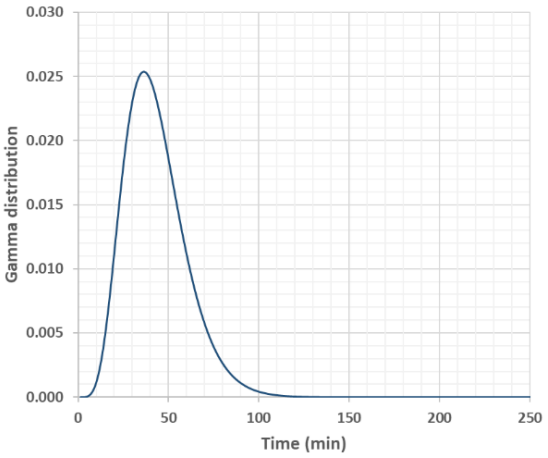

Figure 3. Function $\rho(t)$ obtained from the *AM-VBTA* polymerization reaction. This distribution reached a mean value $m = 43.0$ min and a size distribution $\sigma = 16.8$ min (see Table 5).

Table 5. Parameters of the gamma distribution function, $\rho(t)$, Equation (4), determined by the minimization of the mean square deviation between experimental excess heat flow data and Equation (3).

Copolymer	m [min]	σ [min]
AM-VBTA	43.04	16.84
VBTA-VP	86.93	50.16
VP-AM	107.1	57.82

The second function in Equation (3) is $Q(t)$, which describes the mean heat generated by the chemical reaction on a monomer with a free radical. This function was modeled with Equation 7.

$$Q(t) = A\,(\dot{p}(t) + B\,t\,\ddot{p}(t))^n \tag{7}$$

where A, B, and n represent the parameters. Meanwhile, $\dot{p}(t)$ and $\ddot{p}(t)$ denote the time derivative and second time derivative of the function $p(t)$, respectively. The average heat produced by the reaction of monomers with free radicals depends on the reaction velocity (linked to $\dot{p}(t)$) and its acceleration (linked to $\ddot{p}(t)$). Equation (7) provides a plausible assumption for this unknown function. Additionally, the function $p(t)$ describes the total monomer conversion in the system and is modeled with

$$p(t) = \sum_{\alpha} x_\alpha\; p_\alpha(t) \tag{8}$$

where $p_\alpha(t)$ is the monomer conversion function in Equation (1), and x_α is the molar fraction in the binary mixture. In short, the model for describing the excess heat flow is Equation (3). This model is based on the convolution of two contributions: the distribution $\rho(t)$ and the mean heat generated from the chemical reaction, $Q(t)$. All the parameters in this model belong to the set $S = \{A,\ B,\ n,\ m,\ \sigma\}$, their values are displayed in Tables 5 and 6 and were computed by using a minimization procedure applied in the square

Table 6. Parameter values in the mean heat flow, $Q(t)$, Equation (8), determined by the minimization of the mean square deviation between experimental excess heat flow data and Equation (3).

Copolymer	A [mW]	B [min^{-1}]	n
AM-VBTA	1.241	0.07226	0.2691
VBTA-VP	3.316	0	1
VP-AM	3.367	0	1

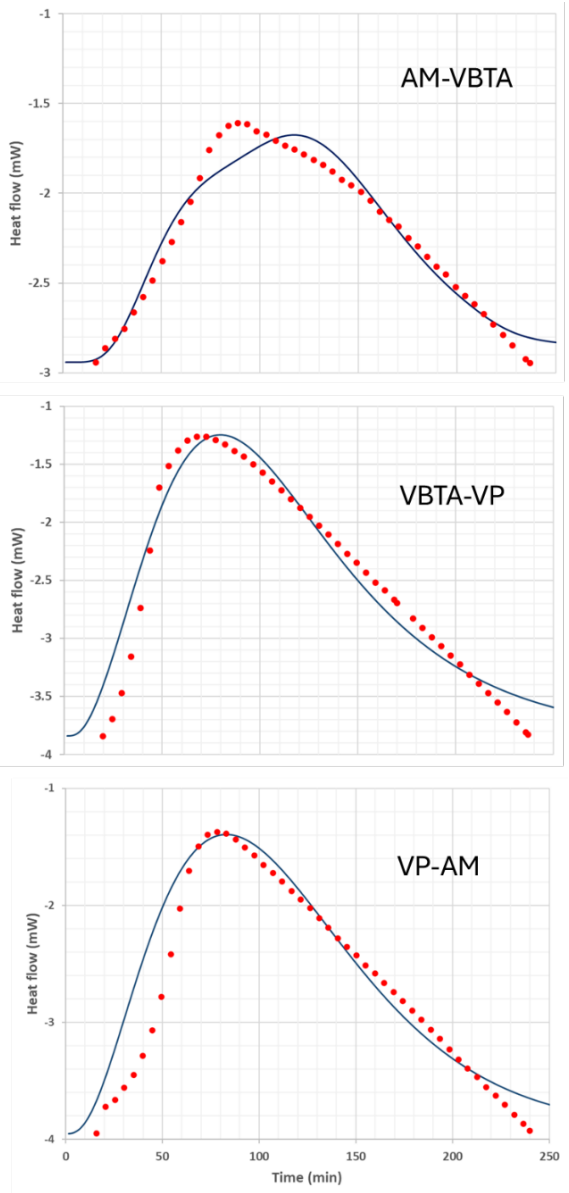

Figure 4. Heat flow $q(t)$ obtained from the *AM-VBTA*, *VBTA-VP*, and *VP-AM* polymerization reactions. The solid curve is the result of $\Delta q(t) + q_{base}(t)$ and the experimental data are red dots.

mean deviation of the excess heat flow $\Delta q(t)$ derived from experimental data and Equation (3).

3.3 Results

Employing the DSC technique, the heat flow of the three copolymerization systems was quantitatively determined. For the copolymerization system *AM-VBTA*, the maximum energy peak was observed at 88.8min, accompanied by a heat flow of -1.61mW. Similarly, for the copolymer *VBTA-VP*, the maximum heat flow of -1.26mW was recorded at 67.7min. Lastly, for the copolymer *VP-AM*, the maximum heat flow of -1.38mW was observed at 78.3min. The experimental data are presented in Figure 3, with red dots. The solid line in Figure 4 represents the heat flow model, specifically Equation (3) plus the baseline, namely: $q(t) = \Delta q(t) + q_{base}(t)$. This model captured the average characteristics of experimental data. However, it exhibited a deviation at the end of the window time in all instances. In contrast, the *AM-VBTA* model exhibited a maximum peak to the right of the experimental data. Furthermore, the experimental data exhibited intricate behavior patterns, potentially suggesting a multimodal distribution of monomers with a free radical.

Conclusions

By employing the ^{1}H NMR monitoring methodology outlined in the experimental design, it was feasible to ascertain the conversion percentage for the diverse copolymer systems. Utilizing the in-situ ^{1}H NMR technique, the reaction progression was quantified by monitoring the signals associated with vinyl groups of the monomers, thereby analyzing the pairwise polymerization systems (copolymers).

The monomer conversions function into polymers during the polymerization reaction, namely $p_\alpha(t)$, whose data are derived from ^{1}H NMR experiments, are accurately described with Equation (1). However, Equation (1) could be improved by adding more terms to describe the multimodal behavior of *VP* in Figure 2 (polymer *VP-AM*). In contrast, for heat flow data obtained using the DSC technique, it was concluded that the correlation Equation (3), namely $\Delta q(t)$, that is based on a density of monomers with a free radical, and this distribution is modeled using a Gamma-type distribution and validated for time $t \geq 0$ by employing the baseline of each system. In general, an acceptable correlation between the heat flow derived from experimental data and the model, with an overall error of less than 15%, was observed. Finally, the model was developed for polymerization reactions using inverse microemulsions, but it is also sufficiently general to apply to conventional polymerization reactions.

Acknowledgements

The authors acknowledge the support by the Instituto Mexicano del Petróleo to carry out the present research work through the project D.62013.

References

Abramowitz, M.; Stegun, I.A.; (1972). *Handbook of mathematical functions*, Dover publication, NY. URL: https://digital.library.unt.edu/ark:/67531/metadc40301/.

Adumitrăchioaie, A.; Tertiş, M.; Cernat, A.; Săndulescu, R.; Cristea, C.; (2018). Electrochemical Methods Based on Molecularly Imprinted Polymers for Drug Detection. *International journal of electrochemical science*; **13** (3), 2556-2576. DOI: https://www.doi.org/10.20964/2018.03.75.

Alb, A. M., Farinato, R., Calbick, J., & Reed, W. F. (2006). Online Monitoring of Polymerization Reactions in Inverse Emulsions. *Langmuir*, **22**(2), 831-840. DOI: https://www.doi.org/10.1021/la051891x.

Bai, Baojun; Zhou, Jia; Yin, Mingfei; (2015). A comprehensive review of polyacrylamide polymer gels for conformance control. *Petroleum Exploration and Development*; **42** (4), 525-532. DOI: https://www.doi.org/10.1016/S1876-3804(15)30045-8.

Choonara, Y.E.; Pillay, V.; Ndesendo, V.M.K.; du Toit, L.C.; Kumar, P.; Khan, R.A.; Murphy, C.S.; Jarvis, D.-L.; (2011). Polymeric emulsion and crosslink-mediated synthesis of superstable nanoparticles as sustained release anti-tuberculosis drug carriers. *Colloids and Surfaces B: Biointerfaces*; **87** (2), 243-254. DOI: https://www.doi.org/10.1002/bdd.750.

Colmán, M.M.E.; Ambrogi, P.M.N.; Serra, C.S.R.; Araujo, P.H.H.; Sayer, C.; Giudici, R.; (2016). At-Line Monitoring of Conversion in the Inverse Miniemulsion Polymerization of Acrylamide by Raman Spectroscopy. *Ind. Eng. Chem. Res.*; **55** (22), 6317-6324. DOI: https://www.doi.org/10.1021/acs.iecr.6b00571.

Colmán, M. M. E.; Chicoma, D. L.; Giudici, R.; Araújo, P. H. H.; Sayer, C.; (2014). Acrylamide

inverse miniemulsion polymerization: in situ, real-time monitoring using nir spectroscopy. *Braz. J. Chem. Eng.*; **31** (4), 925-933. DOI: https://www.doi.org/10.1590/0104-6632.20140314s00002719.

Gu, Qiang; Lin, Quan; Hu, Chunling; Yang, Bai; (2005). Study on Emulsion and Suspension In Situ Polymerization. *J. Appl. Polym. Sci.*; **95** (2), 404-412. DOI: https://www.doi.org/10.1002/app.21401.

D. Guzmán-Lucero, J. F. Palomeque-Santiago, A. Vega-Paz, J. Guzmán-Pantoja, N. V. Likhanova, F. J. Guevara-Rodríguez; (2024). Dosage of monomers in a polymerization reaction. *Rev. Mex. Ing. Quím.*, **23**, Poly24316. DOI: https://www.doi.org/10.24275/rmiq/Poly24316.

Hassan, Saleh F.; Han, Ming; Zhou, Xianmin; Krinis, Dimitrios; Zahrani, Badr; (2013). Study of Polyacrylamide/Cr III Hydrogels for Conformance Control in Injection Wells to Enhance Chemical Flooding Process. *OnePetro*, DOI: https://www.doi.org/10.2118/168069-MS

Hamzehlou, Shaghayegh; Asua, José Maria; (2020). *On-line monitoring and control of emulsion polymerization reactors @ Advances in Chemical Engineering*. Academic Press; **56** (1), 31-57. ISBN 9780128206454 DOI: https://www.doi.org/10.1016/bs.ache.2020.07.002.

Jung, Jae Chul; Zhang, Ke; Chon, Bo Hyun; Choi, Hyoung Jin; (2013). Rheology and polymer flooding characteristics of partially hydrolyzed polyacrylamide for enhanced heavy oil recovery. *J. Appl. Polym. Sci.*; **127** (6), 4833-4839. DOI: https://www.doi.org/10.1002/app.38070.

Ferguson, J.; Sundar Rajan, V.; (1979). The hydrolysis of *N*-vinylpyrrolidone in the presence of polyacrylic acid and potassium persulphate. European Polymer Journal; **15** (7), 627-630. DOI: https://www.doi.org/10.1016/0014-3057(79)90087-9.

Giles, Harold F.; Wagner, John R.; Mount, Eldridge M; (2005). *Chapter 18 - Polymer Overview and Definitions.* William Andrew Publishing, 165-177, ISBN 9780815514732. DOI: https://www.doi.org/10.1016/B978-081551473-2.50019-2.

Gaillard, N.; Giovannetti, B.; Favero, C.; (2010). Improved Oil Recovery using Thermally and Chemically Protected Compositions Based on co- and ter-polymers Containing Acrylamide. OnePetro, DOI: https://www.doi.org/10.2118/129756-MS.

Hao, J.; Song, A.; Wang, J.; Chen, X.; Zhuang, W.; Shi, F.; Zhou, F.; Liu, W.; (2005). Self-assembled structure in room-temperature ionic liquids. *Chemistry - A European Journal*; **11** (13), 3936-3940. DOI: https://www.doi.org/10.1002/chem.200401196.

Ianchis, R.; Donescu, D.; Cinteza, L.O.; Purcar, V.; Nistor, C.L.; Petcu, C.; Nicolae, C.A.; Gabor, R.; Preda, S.; (2014). Polymer-clay nanocomposites obtained by solution polymerization of vinyl benzyl triammonium chloride in the presence of advanced functionalized clay *J. Chem. Sci.*; **126** (3), 609-616. DOI: https://www.doi.org/10.1007/s12039-014-0621-0

Li, Shaofen; (2017). *Chapter 12 - Fundamentals of Polymerization Reaction Engineering @ Reaction Engineering*. Butterworth-Heinemann, 541-598, ISBN 9780124104167. https://www.educate.elsevier.com/book/details/9780124104167.

Lu, Jianmei; Yan, Feng; Texter, John; (2009). Analysis of Bacterial Cellulose/Ionic Liquid MWCNTs via Cyclic Voltammetry. *Progress in Polymer Science*; **34** (5), 431-448. DOI: https://www.doi.org/10.1016/j.progpolymsci.2008.12.001.

Mazrouaa, A.; Badawi, A.; Mansour, N.; Fathy, M.; Elsabee, M.; (2013). Preparation of emulsion Polymerization from Styrene Vinylpyrrolidone and Studying ther Thermal Stability and Electrical Conductivity. *Journal of Nano- and Electronic Physics*, **5** (4), 04063. DOI: https://www.doi.org/2077-6772/2013/5(4)04063(5).

Moghaddam, M. M., & Ramazani Saadatabadi, A. (2025). Modeling and Experimental Survey on Inverse Emulsion terpolymerization of Acrylamide, Styrene and Maleic anhydride as Associative Amphiphilic Polymer. *J. Mol. Liq.*, **424**, 127044. DOI: https://www.doi.org/10.1016/j.molliq.2025.127044.

Namazi, Hassan; (2017). Polymers in our daily life. *Bioimpacts*; **7** (2), 73-74. DOI: https://www.doi.org/10.15171/bi.2017.09.

Noppakundilograt, S.; Nanakorn, P.; Jinsart, W.; Kiatkamjornwong, S.; (2010). Synthesis of acrylamide/acrylic acid-based aluminum

flocculant for dye reduction and textile wastewater treatment. *Polym. Eng. Sci.*; **50** (8), 1535-1546. DOI: https://www.doi.org/10.1002/pen.21694.

Qiu, Zhiming; Texter, John; (2008). Ionic liquids in microemulsions. *Current Opinion in Colloid & Interface Science*; **13** (4), 252-262. DOI: https://www.doi.org/10.1016/j.cocis.2007.10.005.

Sadeghalvaad, Mehran; Sabbaghi, Samad; (2015). The effect of the TiO2/polyacrylamide nanocomposite on water-based drilling fluid properties. *Powder Technology*; **272**, 113-119. DOI: https://www.doi.org/10.1016/j.powtec.2014.11.032.

Sheng, James J.; Leonhardt, Bernd; Azri, Nasser; (2015). Status of Polymer-Flooding Technology**.** *Journal of Canadian Petroleum Technology*; **54** (2), 116-26. DOI: https://www.doi.org/10.2118/174541-PA.

Shrivastava, A.; (2018). *Chapter 2 - Polymerization @ Introduction to Plastics Engineering*. William Andrew Publishing, 17-48. DOI: https://www.doi.org/10.1016/B978-0-323-39500-7.00002-2

Silva, Wandeklebio K.; Chicoma, Dennis L.; Giudici, Reinaldo; (2011). In-situ real-time monitoring of particle size, polymer, and monomer contents in emulsion polymerization of methyl methacrylate by near infrared spectroscopy. *Polym. Eng. Sci.*; **51** (10), 2024-2034. DOI: https://www.doi.org/10.1002/pen.22100.

Singh, Paramjit; Sawhney, Harjot K; (1994). Studies on Copolymerization of Acrylamide and N-Vinylpyrrolidone. *Journal of Macromolecular Science, Part A*; **31** (5), 613-627. DOI: https://www.doi.org/10.1080/10601329409349742.

Singh, P., & Sawhney, H. (1994). Studies on Copolymerization of Acrylamide and N-Vinylpyrrolidone. *J. Macromol. Sci., Part A*, **31**(5), 613-627. DOI: https://www.doi.org/10.1080/10601329409349742.

Stahl, G. A.; Moradi-Araghi, A.; Doe, P. H.; (2024). *High Temperature and Hardness Stable Copolymers of Vinylpyrrolidone and Acrylamide @ Water-Soluble Polymers for Petroleum Recovery*. Springer US, Boston, MA, ISBN 978-1-4757-1985-7. DOI: https://www.doi.org/10.1007/978-1-4757-1985-7_6.

Torraga, M. G. F., Colmán, M. M. E., & Giudici, R. (2021). Mathematical Modeling of Inverse Miniemulsion Polymerization of Acrylamide with an Oil-Soluble Initiator. *Ind. Eng. Chem. Res.*, **60**(43), 15428-15442. DOI: https://www.doi.org/10.1021/acs.iecr.1c02438.

Wang, Xinming; Li, Weiping; Luo, Laihui; Fang, Zhao; Zhang, Jing; Zhu, Yuejin; (2012). High dielectric constant and superparamagnetic polymer-based nanocomposites induced by percolation effect. *J. Appl. Polym. Sci.*; **125** (4), 2711-2715. DOI: https://www.doi.org/10.1002/app.36587.

Xu, Lili; Che, Lixia; Zheng, Jing; Huang, Guangsu; Wu, Xiaorong; Chen, Pengdao; Zhang, Liyu; Hu, Qiaoman; (2014). Synthesis and thermal degradation property study of *N*-vinylpyrrolidone and acrylamide copolymer. *RSC Adv.*; **4** (63), 33269-33278. DOI: https://www.doi.org/10.1039/C4RA05720A.

Yildiz, U., Capek, I., Berek, D., Sarov, Y., & Rangelow, I. W. (2007). Inverse microemulsion copolymerization of butyl acrylate and acrylamide: kinetics, colloidal parameters and some model applications. *Polymer International*, **56**(3), 364-370. DOI: https://www.doi.org/10.1002/pi.2151.